Broadband measurements of transition radiation at Astra-Gemini

Contact *Steffen.Wunderlich@desy.de*

S. Wunderlich, C. A. J. Palmer, J.-P. Schwinkendorf, J. Osterhoff and B. Schmidt
DESY, Notkestr. 85, 22607 Hamburg, Germany

J. Cowley, N. Bourgeois, A. Dyson, G. Cheung, C. Thornton and S. M. Hooker
University of Oxford, John Adams Institute
Clarendon Laboratory, Oxford, OX1 3PU, UK

S. J. Hawkes, N. Booth and D. R. Symes
Central Laser Facility, STFC Rutherford Appleton Laboratory, Chilton, Didcot, OX11 0QX, UK

Introduction

Transition radiation (TR) is generated whenever a charged particle, or bunch of particles, crosses the interface between two materials with different dielectric constants [1]. The properties of this radiation, i.e. spectral and angular intensity, are dependent of the characteristics of the bunch and therefore TR can be used as a bunch diagnostic.

TR is broadband, with the radiation resulting from the individual electrons of the bunch adding with increasing coherence as the wavelength of the radiation exceeds the duration of the bunch. For long bunch durations, typical of many radio-frequency accelerators, the generated TR is incoherent within the optical region of the spectrum. This radiation can be used for measurement of the bunch transverse profile and total charge as the intensity of the incoherent light scales linearly with the charge of the bunch ([2] and references therein). However, microbunching and/or stronger compression leads to coherent emission, which alters the relationship between charge and spectral intensity.

$$\frac{\mathrm{d}^2U}{\mathrm{d}\omega\,\mathrm{d}\Omega} \approx \frac{\mathrm{d}^2U_1}{\mathrm{d}\omega\,\mathrm{d}\Omega}\, N^2\, |F(\omega,\Omega)|^2 \qquad (1)$$

For coherent light, the intensity of the radiation is related not only to the charge of the bunch, through its square, but also to the form factor of the bunch. This is the Fourier transform of the three-dimensional bunch distribution. The relation is shown in equation 1, where the intensity per unit angle per unit bandwidth is expressed in terms of the contribution of a single electron U_1, the number of electrons within the bunch, N, and the square of the modulus of the form factor. It is possible, through measurement of the TR spectrum over a broad wavelength range and calculation of the single particle contribution, to approximate the form factor of the bunch and therefore estimate the longitudinal bunch length [2]. Since a spectrometer provides only a measure of the amplitude of the TR spectrum it is also necessary to determine the wavelength dependent phase of the radiation in order to obtain detailed information about the longitudinal bunch structure.

Laser-driven plasma wakefield accelerators can be used to produce energetic electron bunches with intrinsically short duration (~ fs) due to the limited size of the accelerating structure. For these short bunch lengths coherent TR will be emitted at wavelengths extending down to the NIR and visible region of the spectrum [3]. TR measurements, built up over multiple shots, have already been used to estimate the bunch duration [4]. However, such multi-shot measurements are not suitable for all laser-driven wakefield experiments, many of which lack shot-to-shot stability.

Here we present single-shot measurements of broadband TR spectra, and transverse beam profiles, resulting from the acceleration of self-injected electrons within a laser-driven wakefield at the Astra-Gemini laser facility. While the data presented is preliminary, the outlooks section will discuss several phase retrieval mechanisms. It is planned to use these technique to estimate the phase of the TR and therefore gain more information about the longitudinal bunch structure.

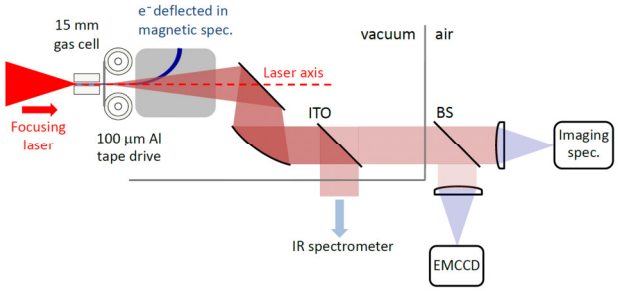

Figure 1. Schematic of the TR setup.

Experimental setup

The experiments described used a 15 mm long capillary target as a gas cell, filled with hydrogen gas or 4% nitrogen-doped hydrogen. The capillaries had a diameter of 300 µm and were machined into sapphire blocks at the University of Oxford.

The South beam of the Astra-Gemini laser was apodised in order to improve the quality of the focal spot. The beam was focussed by an f = 3 m off-axis parabolic mirror to the focus shown in Fig. 2 (top). 41% of the beam energy was contained within the FWHM, compared to the 50% that may be expected for a perfect Gaussian. Radially averaging the profile gives w_0 = 40 µm, with a FWHM of 17 µm (Fig. 2, bottom). The apodisation reduced the on-target energy to a total of 4.1 J – with 1.7 J within the focus FWHM – delivered within a pulse of duration 55 fs, corresponding to an incident peak power of 31 TW within the lowest order mode and a peak intensity of 1.2 x 10^{18} W cm^{-2}.

The target gas was ionised by the front edge of the laser pulse and a plasma wakefield structure was formed inside the gas cell. Electrons were injected into and subsequently accelerated by the wakefield either through the self-injection mechanism in the pure hydrogen target or a combination of self-injection and ionisation injection in the nitrogen-doped target.

Transmitted laser light was reflected from a series of glass wedges to reduce its intensity and sent out of the target chamber to a diagnostics table containing a system to image the laser mode at the exit of the capillary, an optical spectrometer, and a photodiode to measure the transmitted energy. A GRENOUILLE was used separately to measure the laser pulse duration.

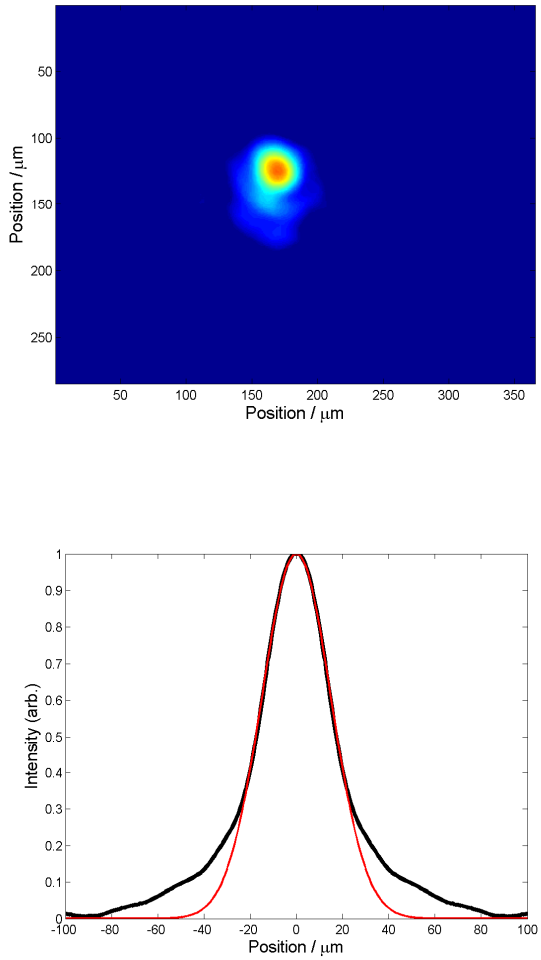

Figure 2. Image of the focal spot (top), together with a plot of the transverse line-out (black line) and a fitted Gaussian of w_0 40 μm (red line).

A two-screen spectrometer was used to measure the electron energy (Fig. 3). Gaining information about the dispersed electron beam position in two planes allows for energy corrections that arise due to pointing variations of the electron beam in the dispersion axis [5]. This adjustment was only partially successful due to the observed shape of the electron spectra.

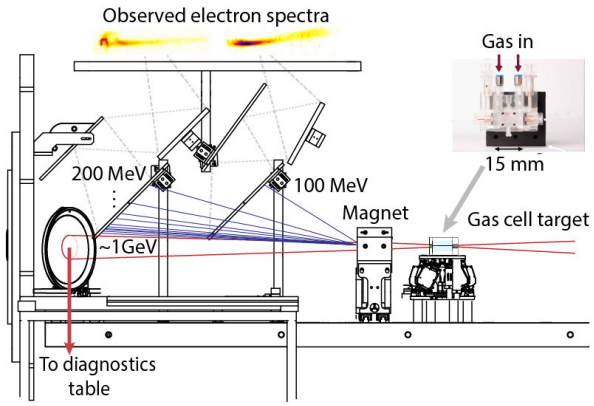

Figure 3. Schematic showing the two screen setup of the electron spectrometer. The laser (red) arrives from the right hand side, and the accelerated electrons (blue) are deflected by a magnet according to their energy. They are then imaged on Lanex sheets.

After exiting the gas cell, the electron bunch propagated 66 mm before passing through a 100 μm thick aluminium foil with a width of 10 mm. This foil generated TR which was collected after the magnet of the electron spectrometer and collimated using a spherical mirror under a small angle. The TR was then split using a thin glass plate with an indium tin oxide (ITO) coating. Here, the NIR ($\lambda > 2$ μm) was reflected through a zinc selenide (ZnSe) window to the infrared prism spectrometer while the transmitted light was directed out of the vacuum via a BK7 window. Following this the visible TR was again split between an imaging spectrometer (Andor Shamrock 303i with Andor Newton DU420A), with a 600 line/mm grating, and an EMCCD (Andor iXon 888). The wavelength range of the spectrometer was from (400 – 1000) nm, although this has been truncated to 700 nm due to strong background in the spectral region of the laser (~ 800 nm).

Infrared Spectrometer setup

Since the slope of the form factor changes dramatically in the mid-infrared [4] for femtosecond electron bunches expected in this experiment, a new double-prism spectrometer for mid-infrared wavelengths has been developed.

The double-prism design allows the measurement of radiation in the wavelength range between (6-18) μm, with a single detector stage due to continuous dispersion without higher orders.

The spectrometer utilises a line array of 128 photo-conductive mercury cadmium telluride (MCT) detector elements attached to a liquid nitrogen dewar, to maintain a temperature of 77 K, for low-noise operation. The detector system shows a sensitivity approximately a factor of 100 higher than that of pyro-electric detectors, which are in use in similar spectrometers for mid- and far-infrared transition radiation [6,7]. In combination with a chain of fast analogue and digital electronics, the detector system allows for single-shot operation at repetition rates up to 50 kHz.

Results: Electron spectra

When averaged over many shots, there is a trend towards a larger amount of charge detected when nitrogen-doped gas is used. We estimate total accelerated charge of (49±44) pC when using nitrogen doped gas, and (27±34) pC when using hydrogen. The shot-to-shot fluctuation of charge in the beam is significant, with up to 149 pC (N_2 doped) and 100 pC (H_2 only) being recorded. In ionization injection [8], electrons are created at a positon in the wakefield which is more favourable for trapping and as a result a greater number of electrons are accelerated compared to the self-injected case. A related phenomenon is the tendency towards more peaked spectra in the self-injected pure hydrogen accelerator, as charge is injected over a shorter distance longitudinally, resulting in a smaller energy spread.

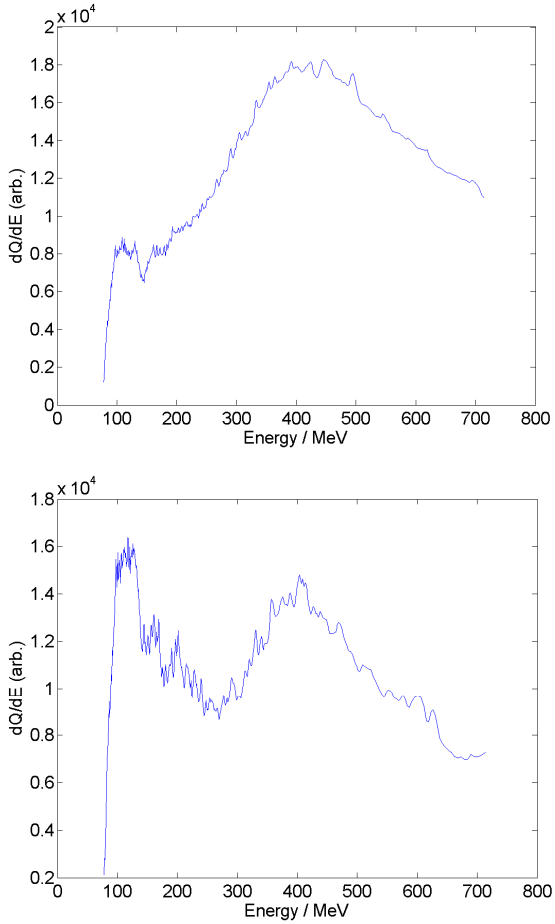

Figure 4. Examples of electron spectra from a pure hydrogen target (top) and hydrogen with 4% nitrogen (bottom). Note the double-peaked spectrum obtained from nitrogen, indicating two electron bunches were accelerated – consistent with intereference occasionally observed in the TR spectrum.

Results: Transition radiation profile

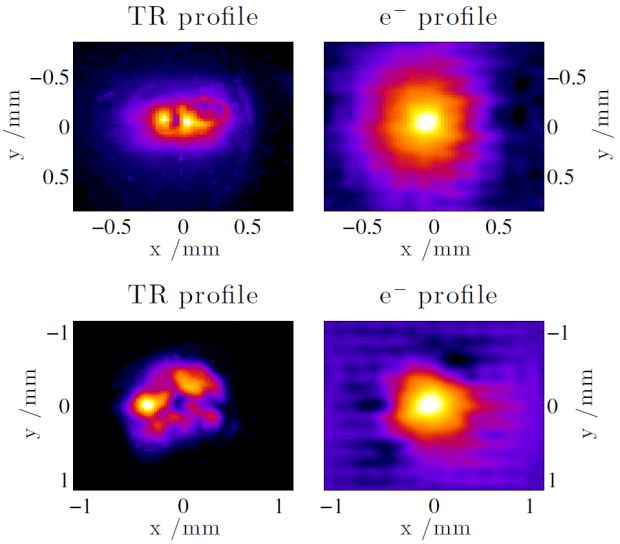

Figure 5. Profile images of transition radiation from two shots (left) with the retrieved electron bunch profile (right). The visible and mid-IR spectra from these shots are shown in figures 6 and 7.

For many shots the TR profile was seen to exhibit the typical ring-like structure of coherent emission [9]. For full transverse coherence, the COTR image represents the gradient of density distribution instead of the density itself. Retrieving the electron bunch profile is still possible; here, the algorithm presented in Ref. [10] was used. This utilises the knowledge that the electron density distribution must be non-zero within a limited range of space and has a positive peak near the middle of the ring of the emission. The reconstruction algorithm proceeds by generating an initial density distribution that is going to be used to calculate an initial intensity profile of the coherent emission. A least-square minimization is performed on the calculated COTR intensity profile in order to obtain a profile that most closely corresponds to the measured COTR intensity profile. Two examples of the TR profile, with the corresponding retrieved electron bunch profile, are presented in Fig. 5.

Results: Transition radiation spectra

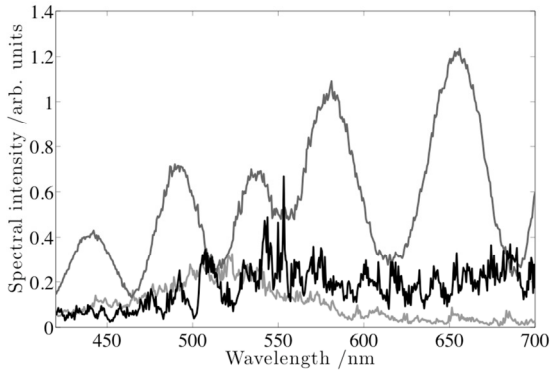

Figure 6. Visible TR spectra from three shots for which the target gas was pure hydrogen. The signal of the regularly modulated spectrum has been reduced by a factor of 10 in order to plot it together with the two weaker spectra.

The visible TR spectra (Figure 6) were seen to fluctuate in intensity and shape. Commonly the spectra exhibited little structure, but in several shots there was evidence of intensity modulation within the spectra. One of these spectra is included in Fig. 6. This could be indicative of interference caused by multiple, temporally-separated electron bunches or substructure within a single bunch. For the example shown this would indicate a separation of approximately 60 fs.

Results: Mid-Infrared Transition radiation spectra

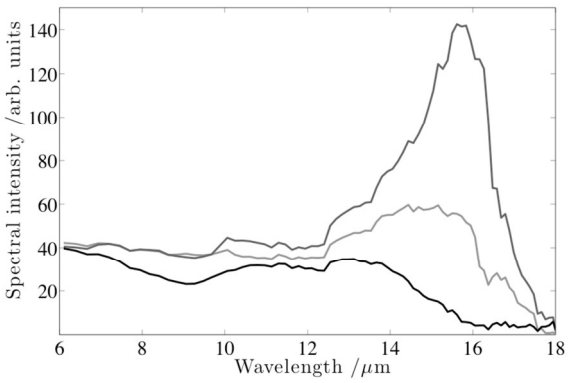

Figure 7. Mid-IR TR spectra from three shots, corresponding to the visible spectra presented in Fig. 6.

Figure 7 depicts preliminary single-shot mid-infrared spectra, measured using the double-prism spectrometer, for three shots. At wavelengths below 10 micron, the signal level is similar for

different shots. On the long wavelength scale, quite significant changes in radiated TR intensity are observable. Due to the studies in progress, the authors have to refer the reader to a future publication, currently in preparation, for a conclusive analysis.

Outlook: Retrieval of a time-domain bunch profile

According to Eqn. (1), the information on the longitudinal shape of the electron bunches is encoded in the spectrum of CTR via the form factor $F(\omega)$. Since the information on the phase in the complex form factor (Eqn. 2) cannot be acquired, a direct determination of the current profile of the electron bunch is not possible.

$$F(\omega) = |F(\omega)| \exp\left(i\Phi(\omega)\right) \quad (2)$$

However, a possible phase can be estimated via mathematical and iterative methods, which qualifies spectroscopy on transition radiation as an attractive and cost-effective method for the longitudinal diagnosis on relativistic electron bunches.

The *Kramers-Kronig* relation provides a mathematical dependency between the real and imaginary part of the Fourier transform for a certain class of functions. The method presented in [2] utilises this relation to calculate the minimal phase and thus, a possible complex form factor and longitudinal current profile.

Alternatively, algorithms have been developed which are based on consecutive Fourier transforms starting from a random phase. This phase is then iteratively adjusted by the stepwise combination of the measured modulus of the form factor and a phase, calculated during the successive transformation between time and Fourier domain [11].

Another method is an extended *Gerchberg-Saxton* algorithm regarding support constraints in time and Fourier domain in a sequence of direct and inverse Fourier transforms. The *Bubblewrap* algorithm [12] additionally includes dynamic adaption of the constraints, thresholds and convergence criteria to deliver a probable time-domain profile.

All the phase-retrieval methods depend on the precise knowledge of the input parameter, i.e. the modulus of the form factor $|F(\omega)|$.

Regarding Eqn. (1), the spectral intensity at the Aluminium foil, acting as the transition radiation source, $dU/d\omega$, has to be determined by considering the transmission of the optical system and the calibration of the spectrometers. In addition, the single-electron contribution, $dU_1/d\omega$, and the number of particles in the bunch, N, have to be calculated analytically and to be measured, respectively.

In order to perform comparative studies utilising the phase retrieval algorithms mentioned above, the absolute calibrations of the spectrometers from the visible to the mid-infrared are currently being determined. In combination with the charge measurements and the transverse beam diagnosis, the on-going studies aim to retrieve a possible longitudinal bunch shape based on the broadband single-shot measurement of transition radiation.

Conclusions

Single-shot, broadband measurements of transition radiation, generated using wakefield accelerated electron bunches, have been made at the Astra Gemini facility. TR profiles and spectra from several shots have been presented, together with charge and energy measurements of the electron bunch. This information will be combined in future analysis pursuing retrieval of the electron bunch temporal and spatial profile.

Acknowledgements

The authors would like to thank the support of the CLF team, without whom this work would not have been possible.
The mid-IR spectrometer setup has been supported by the German Federal Ministry of Education and Research (BMBF) under contract 05K10GU2 and FS FLASH 301.
This work has been supported by funding from the Helmholtz Association, the Alexander von Humboldt-Foundation, the Engineering and Physical Sciences Research Council (Grant No. EP/H011145/1) and by the Leverhulme Trust (Grant No. F/08 776/G).

References

1. Ginzburg and I. M. Frank, J. Phys. USSR **9** 353 (1945)
2. R. Lai and A. J. Sievers, Nucl. Instruments Methods Phys. Res. Sect. A **397**, 221 (1997).
3. Y. Glinec, J. Faure, A. Norlin, A. Pukhov and V. Malka, Phys. Rev. Letts. **98,** 194801 (2007)
4. O. Lundh, J. Lim, C. Rechatin, L. Ammoura, A. Ben-Ismaïl, X. Davoine, G. Gallot, J.-P. Goddet, E. Lefebvre, V. Malka, and J. Faure, Nat. Phys. 7, 219 (2011)
5. B.B. Pollock, J. S Ross, G. R. Tynan, L. Divol, S. H. Glenzer, V. Leurent, J. P. Palastro, J. E. Ralph, C. E Clayton, K. A. Marsh, A. E. Pak, T. L. Wang, C. Joshi, LLNL-PROC-412609 (2009)
6. S. Wesch, B. Schmidt, C. Behrens, H. Delsim-Hashemi, and P. Schmüser, Nucl. Instrum. Methods Phys. Res., Sect. A 665, 40 (2011)
7. T. J. Maxwell, C. Behrens, Y. Ding, A. S. Fisher, J. Frisch, Z. Huang, and H. Loos, Phys. Rev. Lett. 111, 184801 (2013).
8. A. Pak, K. A. Marsh, S. F. Martins, W. Lu, W. B. Mori and C. Joshi, Phys. Rev. Lett. **104**, 025003 (2010)
9. H. Loos, R. Akre, A. Brachmann, F.-J. Decker, Y. Ding, D. Dowell, P. Emma, J. Frisch, S. Gilevich, G. Hays, Ph. Hering, Z. Huang, R. Iverson, C. Limborg-Deprey, A. Miahnahri, S. Molloy, H.-D. Nuhn, J. Turner, J. Welch, W. White and J. Wu, Conf. Proc of 30th International Free Electron Laser Conference 2008.
10. N. Bourgois, M. Heigoldt, W. Rittershofer, A. Popp, K. Khrennikov, S. I. Bajlekov, S. Karsch and S. M. Hooker. AIP Conf. Proc. **1507**, 258 (2012).
11. Pelliccia and T. Sen. ArXiv e-prints, March 2014, 1403.1233
12. S. I. Bajlekov, M. Heigoldt, A. Popp, J. Wenz, K. Khrennikov, S. Karsch, and S. M. Hooker, Phys. Rev. Spec. Top. - Accel. Beams 16, 040701 (2013)